

TGA-FTIR study of the vapors released by triethylamine-acetic acid mixtures

Nontete Suzan Nhlapo^a, Walter W. Focke^{a,*} and Eino Vuorinen^b

^aInstitute of Applied Materials, Department of Chemical Engineering, University of Pretoria,
Private Bag X20, Hatfield 0028, Pretoria, South Africa

^bNational Metrology Institute of South Africa, Private Bag X34, Lynnwood Ridge, Pretoria, South Africa, 0040

ABSTRACT

Proprietary mixtures of amines and carboxylic acids are used as volatile corrosion inhibitors (VCIs) for the protection of iron and steel components against atmospheric corrosion. This study was focused on the nature of the vapors they release. VCI model compounds comprising mixtures of triethylamine and acetic acid were studied using thermogravimetric analysis coupled with Fourier-transform infrared spectroscopy (TGA-FTIR) at 50°C. As vaporization progressed, the composition of the remaining liquid and the emitted vapor converged to a fixed amine content of ca. 27 mole percent. This was just above the composition expected for the 1:3 amine to carboxylic acid complex. Mixtures close to this composition also featured the lowest volatility.

Keywords: Carboxylic acids; Amines, Vapor, TGA-FTIR, VCIs

*Corresponding author: Walter W. Focke, Tel: +27(12) 420 3728; Fax: +27(12) 420 2516

E-mail address: walter.focke@up.ac.za

1. Introduction

Volatile corrosion inhibitors (VCIs), also referred to as vapor phase corrosion inhibitors, form a protective deposit at the metal interface to limit atmospheric corrosion [1-5]. VCIs can be pure compounds or may comprise suitable mixtures of volatile compounds. Commercial products are available as liquids or powders and are supplied in sachet or tablet dosage forms [3]. VCIs are also incorporated in polymeric films and in paper used for packaging metal components [5,9].

VCIs evaporate or sublimate and migrate via the gas phase to the metal surface to be protected [4]. They reach the metal surface by diffusion and render protection following adsorption [7,9]. Experience has taught that the vapor pressure should be in the range 0.002 Pa to 1 Pa at 20 °C for effective VCI transport [3, 7-10]. Too low a vapor pressure leads to slow establishment of protection. High vapor pressures imply high consumption rates and either lead to an early loss of inhibitor activity [7] or limit the effectiveness of VCI to a short period of action [3,7].

Appropriate mixtures of amines and carboxylic acids can provide both short- and long-term protection against metal corrosion during storage and transportation [5,9-11]. This class of VCIs is mainly used for the protection of mild steel and iron [3,9]. The pH should exceed pH = 5.5 to ensure adequate steel protection [3]. Therefore the amine has to be present in the vapour in excess otherwise the mixtures might promote corrosion.

The interactions between amines (A) and carboxylic acids (C) have been comprehensively studied [12-18]. Amines and carboxylic acid mixtures interact strongly via hydrogen bonding

[12,15]. In 1:1 mixtures they form A_1C_1 molecular complexes in the vapor phase [19-30] or ionic complexes in the liquid phase via Brønsted-Lowry acid-base reactions [17]. The A_1C_1 ionic complex requires stabilization and *ab initio* calculations showed that, at equimolar mixing ratios, the formation of an A_2C_2 complex is more likely [17]. In the absence of water and in the presence of excess carboxylic acid, the A_1C_1 complex is stabilized by reacting with the cyclic dimers of the carboxylic acid forming the A_1C_3 complex [12,17,18,21-24]. The formation of the A_1C_3 complex in triethylamine-acetic acid mixtures is supported by the sharp viscosity maximum observed at the 1:3 amine to acid mole ratio [16]. The existence of an A_1C_2 complex has also been reported [12,18,23-24]. When the tertiary amine is replaced with a secondary or a primary amine the situation changes dramatically. The 1:1 complex becomes increasingly important and in the case of primary amines there is a tendency for these to form large clusters [15].

Ternary systems comprising amines and carboxylic acids dissolved in non-ionizing or non-dissociating solvents such as chloroform, carbon tetrachloride and benzene, have been studied as well [25-28]. Near UV absorption studies indicated proton transfer from the carboxylic acids to the amine [29]. This was also theoretically predicted by *ab initio* calculations for the trimethylamine-formic acid and propylamine-propionic acid systems [22,30]. The ionic nature of the complexes was confirmed by both mid and near infrared spectroscopy [20,21,24-25], FT-Raman [17], $^1\text{H-NMR}$ and $^{13}\text{C-NMR}$ [15,31], dielectric spectroscopy, conductivity measurements [18,23], melting and boiling point measurements, ultrasound absorption and relaxation spectroscopy [12,24,32-33], and combinations of different measurement techniques including density, optical refractive index, and shear viscosity [23].

Kubilda and Schreiber [19] conducted FTIR studies of the vapors of trimethylamine mixtures with acetic acid and trifluoroacetic acid at high temperatures. However, there is little literature on the nature of the vapors emitted by VCIs. Hence the aim of the present study was to develop a practical TGA-FTIR method to determine the composition of the vapors released by amine-carboxylic acid mixtures VCI model compounds as a function of time. Triethylamine-acetic acid mixtures were used to validate the method because much data are available for this system.

2. Experimental

2.1. Reagent

Acetic acid (99.8%), triethylamine (TEA) (99%), silica gel and sodium bicarbonate were supplied by Merck chemicals. Drierite 8 mesh drying agent was supplied by Sigma Aldrich. All the reagents were used as received without further purification.

2.2. Method

TEA-acetic acid binary mixtures were prepared in a dry glove box under a nitrogen atmosphere to avoid air oxidation or contamination with moisture. TEA-acetic acid binary mixtures were prepared by weighing out predetermined amounts of the constituents. All the experiments were performed at an atmospheric pressure of 91.6 ± 0.3 kPa. Phase separated TEA-acetic acid mixtures were individually characterized and labelled top or bottom depending on the position of the phase separated layer.

Liquid-liquid phase composition data was determined by the titration method under reflux at atmospheric pressure. TEA was added to a known amount of acetic acid at 50 °C from a burette until the mixture became cloudy. The temperature of the mixture was controlled by water bath. The experiment was repeated at least four times for statistical purposes.

2.3. Instrumentation

The binary mixtures were characterized using simultaneous thermogravimetric analysis Fourier-transform infrared spectroscopy (TGA-FTIR). Data was collected on a Perkin-Elmer TGA 4000 thermogravimetric analyzer coupled with Spectrum RX 100 spectrometer with a 1 m TL800 EGA transfer line. A 180 μ l open alumina pan was partially filled with 85 ± 5 mg of sample. The sample was heated from 25 °C to 50 °C, at heating rate of 20 °C min^{-1} and kept isothermal at 50 °C for the duration of the test period. The high test temperature of 50 °C was selected to maximize volatility and because it corresponds to the highest temperature VCI's are expected to function during commercial use. The data was collected under N_2 at the flow rate of 50 mL min^{-1} to prevent oxidation. The evolved gases were transferred from the TGA to FTIR cell at a flow rate of 30 mL min^{-1} . The spectra were recorded every minute at 2 cm^{-1} wavenumber intervals at a resolution of 2 cm^{-1} . The transfer line and FTIR cell temperature were both kept at 230 °C to avoid condensation and to dissociate all complexes.

There is a time lag from the point where vapors are released and recorded as a TGA mass loss signal and the capture of the corresponding FTIR spectrum. The length of this time delay was determined experimentally by monitoring the thermal decomposition of sodium bicarbonate. This reaction releases carbon dioxide which features a strong IR absorption band at 2349 cm^{-1} . Approximately 30 mg of sodium bicarbonate was placed in an open 180 μ l alumina pan. The sample was heated from 25-400 °C at 20 °C min^{-1} in N_2 gas at flow rate of 50 mL min^{-1} .

The delay time was determined as the time difference between the times for the TGA derivative mass loss signal reached a maximum and the maximum absorption of the CO₂ IR peak was reached.

Liquid phase FT-IR data were collected using a Perkin-Elmer Spectrum RX 100 spectrometer. Samples were placed between two KBr crystal windows (25 mm diameter and 4 mm thick). Background corrected spectra were recorded at room temperature in the wavenumber range 4000 to 800 cm⁻¹ at a resolution of 2 cm⁻¹.

Differential scanning calorimetry (DSC) was performed on a Mettler Toledo DSC1 instrument. Approximately 5-10 mg samples were placed in standard 40 µl aluminum pans with a pin hole and heated from -40°C to 400 °C at a heating rate of 10 °C min⁻¹ in nitrogen gas flowing at 50 mL min⁻¹.

3. Results and discussion

Fig. 1 shows the phase diagram for TEA-acetic acid mixtures at 1 atmosphere using the overall amine mole fraction (z_A) as composition descriptor. It summarizes previously reported liquid-liquid equilibrium (LLE) and vapor-liquid equilibrium (VLE) phase composition data for TEA-acetic acid mixtures [12,32]. The LLE data of Kohler and coworkers [12] and van Klooster and Douglas [32] deviate at higher amine concentrations. The LLE data points determined in this study at a temperature of 50 °C ($z_A = 0.44$ and 0.89) are plotted for comparison. They are in better agreement with the values reported by van Klooster and Douglas [32].

3.1. Liquid phase FTIR results

The liquid phase FTIR spectra of acetic acid, TEA and the selected binary mixtures are compared in Fig. 2. Pure acetic acid ($z_A = 0$) shows a sharp and strong intensity absorption band due to carbonyl C=O dimer form at 1705 cm^{-1} , whilst the monomer contribution is observed as a very weak band at 1760 cm^{-1} [34]. A broad and weak intensity band at 944 cm^{-1} is due to the OH out of plane deformation vibration mode of the two hydrogen atoms in the acetic acid dimer ring [35]. The presence of the aforementioned band suggests that acetic acid dimers are the dominant species in the liquid phase. The methyl CH_3 asymmetric and symmetric bending vibration bands are observed at 1409 cm^{-1} and 1360 cm^{-1} [34], respectively. The position of these methyl bands coincides with that of COH in plane bending vibration at 1409 cm^{-1} and a shoulder at 1366 cm^{-1} . The OH deformation vibration is observed at 1051 cm^{-1} coinciding with methyl CH_3 rocking mode and the C=O stretching mode calculated to the value of 1021 cm^{-1} [35]. The shoulder at 1240 cm^{-1} is due to CO stretching vibration [34].

TEA ($z_A = 1.00$) shows an absorption band at 1477 cm^{-1} due to CH_3 anti-symmetric deformation mode. The CH_3 symmetric umbrella deformation mode is observed at 1385 cm^{-1} . The CN stretching vibration mode is observed at 1212 cm^{-1} and 1057 cm^{-1} [34,37].

Addition of amine results in a shift in the dimer C=O band position to higher frequencies and the disappearance of the dimeric OH out of plane deformation band. The lack of the OH out of plane dimer form indicates the absence of dimers and the formation of a complex between acetic acid and TEA [38]. The carbonyl C=O is observed at 1722 cm^{-1} in all TEA-acetic acid mixtures. The contribution due to C=O monomer form is observed as a shoulder in the

mixture with composition $z_A = 0.20$ but is absent when $z_A = 0.33$. The new absorption band is observed at 1576 cm^{-1} is due to the ionic carboxylate, COO^- [20-21]. The COH in plane bending absorption bands shifted position to lower frequency of 1378 cm^{-1} due to hydrogen bonding between acetic acid and TEA observed in all mixtures. The CO stretching absorption band is observed at 1248 cm^{-1} . The intensity of the aforementioned band is stronger compared to acetic acid. The reason for this is attributed to the contribution of CN stretching mode from amine which also occurs at the same position [37]. The bottom phase of the sample prepared as $z_A = 0.80$ shows absorption bands similar to $z_A = 0.20, 0.25$ and 0.33 .

3.2. DSC results

DSC data for acetic acid showed two thermal transitions (see Fig. 3). The first was the melting transition and had an onset of $11\text{ }^\circ\text{C}$ while the second was a (boiling) transition with an onset of $108\text{ }^\circ\text{C}$. TEA melts at $-115\text{ }^\circ\text{C}$. Consequently, in the temperature range studied presently, TEA showed only a single thermal (boiling) transition with an onset temperature of $84\text{ }^\circ\text{C}$. TEA-acetic acid mixtures featured significantly higher boiling transitions when evaporated into a stream of nitrogen gas. A sample with $z_A = 0.39$ and mixture with $z_A = 0.33$ featured onset temperatures of $156\text{ }^\circ\text{C}$. Mixtures with compositions $z_A = 0.20$ and $z_A = 0.25$ showed boiling onsets occurring at $154\text{ }^\circ\text{C}$ and $158\text{ }^\circ\text{C}$ respectively. This suggests that the mixtures with the highest apparent boiling points are those that closely match the composition of the A_1C_3 complex, i.e. an amine to acid mole ratio of 1:3.

3.3. TGA-FTIR

Fig. 4 illustrates how the lag time between the mass loss and FTIR signals was determined. It shows plots of the TG derivative mass loss signal and a plot of the maximum absorbance of

the band located near 2300 wavenumbers in the FTIR spectrum. The excellent match of the superimposed signals was obtained by an appropriate time shift of the former signal. The average lag time was determined as 0.56 ± 0.03 .

Fig. 5 shows TGA mass loss curves for TEA-acetic acid and selected mixtures. Fig. 6 plots the time to reach selected fractional mass loss values as a function of initial mixture composition. The pure compounds evaporated much more rapidly than the mixtures (Figs. 5 and 6). Mass loss was fastest for TEA reflecting its higher volatility compared to acetic acid. Interestingly the $z_A = 0.24$ mixture was the least volatile as it showed the lowest mass loss rate. This composition is close to that of the A_1C_3 complex. The sample of the top layer phase with $z_A = 0.89$ evaporated at a similar rate than pure triethylamine suggesting that mainly the amine was released. The sample with $z_A = 0.39$, with a composition matching that of the bottom layer obtained following phase separation, evaporated at an intermediate rate.

Figs. 7 and 8 compare vapor phase FTIR spectra of representative TEA-acetic acid mixtures to spectra obtained for pure TEA and pure acetic acid vapors. Consider the spectra in Fig. 7 for mixture with composition $z_A = 0.20$. The spectrum recorded when just 3% had evaporated is nearly identical to that for pure TEA. The C=O monomer and OH absorption bands for acetic acid at 1790 cm^{-1} and 1814 cm^{-1} ; and 3580 cm^{-1} , respectively are only noticeable at a much later stage. Consider next the spectra in Fig. 8 for the mixture with initial composition $z_A = 0.33$. Now it appears that it is acetic acid that evaporates initially as the TEA absorption bands are only observed at much later times. This implies that the steady state vapor composition lies between these two compositions.

The dominant features that distinguish the FTIR spectra for TEA and the spectra for acetic acid are the group of bands between 3300 cm⁻¹ and 2450 cm⁻¹ and those between 1950 cm⁻¹ and 1600 cm⁻¹ respectively. These were used to determine the composition of the vapor streams in the following way. The areas under the absorbance vs. wavenumber plots, from 3300 cm⁻¹ and 1600 cm⁻¹ were determined using fourth order Newton Cotes integration [39]. However, interfering CO₂ absorption bands are found in the region between 2270 cm⁻¹ and 2450 cm⁻¹ and this region was therefore excluded from the integration range. The integrated areas scaled directly with the TG mass loss rates according to

$$a_i = k_i \dot{m}_i = \int_{1600}^{2270} A d\sigma + \int_{2450}^{3300} A d\sigma \quad (1)$$

where a_i is the integrated area under the absorbance curve (in the wavenumber ranges indicated) in cm⁻¹, \dot{m}_i is the TGA mass flux of component i entering the vapor phase in mg.min⁻¹, k_i is a characteristic constant for component i with units min.mg⁻¹.cm⁻¹, A is the dimensionless absorbance and σ is the wave number measured in cm⁻¹. The proportionality constants for the instrument combination used in this study were experimentally determined as $k_A = 20.0 \pm 0.2$ and $k_C = 18.3 \pm 0.4$ for triethylamine and acetic acid respectively.

A characteristic normalized shape function for each of the pure components was defined by the following integral

$$\alpha_i(\sigma) = \int_{\sigma}^{3300} A d\sigma / \left(\int_{1600}^{2270} A d\sigma + \int_{2450}^{3300} A d\sigma \right) \quad (2)$$

where the symbols have the same meaning as in Equation (1) with the integral in the numerator excluding the wavenumber range 2270 cm⁻¹ to 2450 cm⁻¹. This shape function

defines the profile of the integrated absorbance as a function of the wavenumber σ . The shape function profile for pure components is independent of the mass flux and this was confirmed experimentally. The shape function profiles for triethylamine and acetic acid are shown in Fig. 9.

Next consider the (normalized) shape function expected for a mixed vapor composition. Van Klooster and Douglas [32] previously found that no molecular interaction occur at 162 °C in the TEA-acetic acid system. The present vapor phase spectra were recorded at an even higher temperature and both components should therefore be present in their monomer forms. Indeed, all the FTIR spectra recorded at 230 °C for the mixtures in this study were consistent with this assumption. The absence of the carbonyl C=O dimer band at 1705 cm^{-1} ; the shape and position of OH band at 3580 cm^{-1} , and the strong C=O absorption band at 1790 cm^{-1} , in the spectrum recorded for the pure acetic acid vapors, confirmed that acetic acid was predominantly present in the monomer form and that the contribution from dimers was insignificant. The ionic carboxylate bands were absent in the vapor spectra obtained for the mixtures. Furthermore, in the mixtures the acetic acid C=O absorption band was observed at the exact same position found for the neat acetic acid (1790 cm^{-1} and 1814 cm^{-1}). This confirmed negligible interaction between acetic acid molecules and TEA molecules in the vapor phase at 230°C.

The absence of complex-forming interactions in the vapor phase at measurement temperature that was used means that the recorded spectra are simply a combination of the spectra expected for the pure compounds. Thus the shape function for a mixed vapor is given by a linear combination of the two pure component shape functions

$$\alpha_{mix} = \beta_{mix}\alpha_A + (1 - \beta_{mix})\alpha_C \quad (3)$$

where β_{mix} is a characteristic measure of the mixture composition and α_A and α_C are the shape functions for triethylamine and acetic acid respectively. The β_{mix} values were determined from experimental data using least square data fits of Equation (3). Once the β_{mix} values were known, the mass fraction amine in the vapor phase was calculated using

$$w_A = \frac{\beta_{mix}}{\beta_{mix} + \frac{k_A}{k_C}(1 - \beta_{mix})} \quad (4)$$

where w_A is the mass fraction of an amine in the vapor. The mole fraction of amine in the vapour (y_A) was determined as follows

$$y_A = \frac{w_A/M_A}{w_A/M_A + (1 - w_A)/M_C} \quad (5)$$

where M_A is the molar mass of component triethylamine and M_C is the molar mass of acetic acid.

Fig. 9 compares the measured shape functions α for pure acetic acid, pure TEA and the vapour released by a specific mixture. As mentioned above, such plots were used to determine the composition of the vapors. This was done by first extracting the β_{mix} values in Equation (3). Next the amine mole fraction in the released vapor was determined by applying Equation (4) and Equation (5). These were then plotted against time (Fig. 10) or against the mass fraction of mixture released (Fig. 11).

Figs. 10 and 11 show that the mole fraction amine in the released vapor (y_A) initially either increases or decreases but then stabilizes at a plateau value. This value is, within experimental error, the same for all mixtures irrespective of their initial concentration. The

plateau composition was determined as $y_A = 0.27 \pm 0.02$ by averaging all the vapor compositions measured beyond the point where 50 % of the original charge had volatilized for mixtures initially containing 19, 20, 23, 24 and 38 mole % TEA. This value is only slightly higher than the composition of the A_1C_3 complex.

When the composition of the emitted vapor stabilizes at a plateau value it must mean that this should also be true for the liquid phase. In fact, the compositions of the vapor and liquid phase should be the same. This can be checked by performing a mass balance. The differential equation is

$$\frac{dm_A}{dm} = \frac{1}{m} \frac{dm_A}{dt} = y_A \quad (6)$$

and

$$\frac{dm_C}{dm} = 1 - y_A \quad (7)$$

where m_i is the mass of component i in the liquid phase. These two equations can be solved by numerical integration using the TGA mass loss data and the vapor phase composition determined from the FTIR results. The mole fraction amine in the liquid phase can then be determined from

$$x_A = \frac{m_A/M_A}{m_A/M_A + (1 - m_A)/M_C} \quad (8)$$

The results of these calculations are presented in Fig. 12. They confirm that the liquid compositions also approached the same plateau value as found for the vapor phase. This indicates that over time, evaporation of an amine-acetic acid mixture will reach an azeotrope-like point where the relative concentrations of the vapor and liquid phases become identical.

The present results indicate that the steady state composition of the vapor released by TEA-acetic acid binary mixtures contains excess acetic acid. When this vapor comes in contact with the absorbed moisture on the surface of a metal, the acid dimers in the A_1C_3 complex will dissociate and hydrolyze to form free monomeric acids that may lower the pH of the water film to values that may induce corrosion [3]. This may provide an explanation as to why TEA-acetic acid is a poor VCI [9]. An effective VCI vapor has to contain excess amine and should not result in too low pH for the liquid water film adsorbed on the metal surface.

4. Conclusions

Volatile corrosion inhibitors (VCIs) are used to prevent atmospheric corrosion of metals. Proprietary mixtures of amines and carboxylic acids are suitable for the protection iron and steel components. The interactions between these two types of molecules are well established but little is known about the nature of the vapors that are emitted. A new method, based on thermogravimetric analysis coupled with evolved gas Fourier transform infrared spectroscopy (TGA-FTIR), was developed in order to shed light on this aspect. The TGA provided information on the rate of VCI release while the FTIR spectra allowed quantification of the composition of the vapor emitted. The method was applied to study a VCI model system based on mixtures of triethylamine and acetic acid. The mixtures were held isothermally at 50 °C and allowed to vaporize into a stream on nitrogen gas in a TGA-FTIR instrument. The vapor phase FTIR spectra were recorded at 230 °C as, at this temperature, interactions between the carboxylic acid and amine molecules were insignificant and little or no dimerization of the carboxylic acids occurred. Irrespective of the initial mixture composition, the composition of the remaining liquid and the emitted vapor settled on the same fixed

steady state value reminiscent of azeotrope behavior. The composition of this plateau value was approximately 27 mole % TEA which is very close to the composition of the stable 1:3 mole ratio amine-acid complex. This vapour composition is rich in acetic acid and this probably explains why TEA-acetic acid mixtures are poor VCIs for mild steel. Interestingly, it was also found that mixtures with compositions close to this value featured the lowest volatility. It is hoped that this method will find utility in the characterization of other VCIs and thereby provide an aid towards understanding their mechanism of action.

Acknowledgements

Financial support for this research, from the National Metrology Institute of South Africa (NMISA), the Institutional Research Development Programme (IRDP) of the National Research Foundation of South Africa, and Xyris Technology CC is gratefully acknowledged.

References

- [1] W. Skinner, A new method for quantitative evaluation of volatile corrosion inhibitors, *Corros. Sci.* 35 (1993) 1494-1501.

- [2] L. R. M. Estevão, R. S. V. Nascimento, Modifications in volatilization rate of volatile corrosion inhibitors by means of host-guest systems, *Corros. Sci.* 43 (2001) 1133-1153.

- [3] D. M. Bastidas, E. Cano, E. M. Mora, Volatile corrosion inhibitors: a review, *Anti-Corros. Methods Mater.* 52 (2005) 71-77.

- [4] N. N. Andreev, Y. I. Kuznetsov, Physicochemical aspects of the action of volatile metal corrosion inhibitors, *Rus. Chem. Rev.* 74 (2005) 685-695.
- [5] U. Rammelt, S. Koehler, G. Reinhard, Use of vapor phase corrosion inhibitors in packages for protecting mild steel against corrosion, *Corros. Sci.* 51 (2009) 921-925.
- [6] E. Vuorinen, E. Kálmán, W. Focke, Introduction to vapour phase corrosion inhibitors in metal packaging, *Surf. Eng.* 20 (2004) 281-284.
- [7] N. Pieterse, W. W. Focke,; E. Vuorinen, I. Rácz, Estimating the gas permeability of commercial volatile corrosion inhibitors at elevated temperatures with thermo-gravimetry, *Corros. Sci.* 48 (2006) 1986-1995.
- [8] W. Skinner, F. Du Preez, E. Vuorinen, Evaluation of vapor phase corrosion inhibitors, *Br. Corros. J.* 34 (1999) 151-152.
- [9] E. Vuorinen, W. Skinner, Amine carboxylates as vapour phase corrosion inhibitors, *Br. Corros. J.* 37 (2002) 159-160.
- [10] E. Vuorinen, W. Focke, A new technique to evaluate the volatility of vapour phase corrosion inhibitors (VCIs) and potential VCIs, *Chem. Technol.* (2006) 26.
- [11] H. Kondo, Protic ionic liquids with ammonium salts as lubricants for magnetic thin film media, *Tribol. Lett.* 31 (2008) 211-218.

- [12] F. Kohler, E. Liebermann, G. Miksch, C. Kainz, On the thermodynamics of the acetic acidtriethylamine system, *J. Phys. Chem.* 76 (1972) 2764-2768.
- [13] F. Kohler, P. Hyskens, Some aspects of the structure and interaction potential of hydrogen bonded complexes, *Adv. Molec. Relax. Proc.* 8 (1976) 125-154.
- [14] P. Hyskens, N. Felix, A. Janssens, F. Van den Broeck, F. Kapuku, Influence of the dielectric constant on the viscosity and on the formation of conducting ions in binary carboxylic acidstriethylamine mixtures, *J. Phys. Chem.* 84 (1980) 1387-1393.
- [15] F. Kohler, H. Atrops, H. Kalal, E. Liebermann, E. Wilhem, F. Ratkovics, T. Salamon, Molecular interactions in mixtures of carboxylic acids with amines. 1. Melting curves and viscosities, *J. Phys. Chem.* 85 (1981) 2520-2524.
- [16] F. Kohler, R. Gopal, G. Götze, H. Atrops, M.A. Demiriz,; E. Liebermann,; E. Wilhelm, F. Ratkovics, B. Palagyl, Molecular interactions in mixtures of carboxylic acids with amines. 2. Volumetric, conductimetric, and NMR properties, *J. Phys. Chem.* 85 (1981) 2524-2549.
- [17] S. Karlsson, J. Päivärinta, R. Friman, A. Poso, M. Hotokka, S. Backlund, Characterization of the phase behavior and complexation in heptanoic acid-heptylamime-water system, *J. Phys. Chem. B* 105 (2001) 7944-7949.
- [18] K. Orzechowski, M. Pajdowska, J. Przybylski, J. Gliński, H. A. Kolodziej, Dielectric, acoustic, desimetric and viscosimetric investigations of the tributylamine + propionic acid system, *Phys. Chem. Chem. Phys.* 2 (2000) 4676-4681.

- [19] A. I. Kubilda, V. M. Schreiber, Infrared study of some complexes with a strong hydrogen bond at high and low temperatures, *J. Mol. Struct.* 47 (1978) 323-328.
- [20] M. Wierzejewsha-Hzat, Z. Mielke, H. Ratajczak, Infrared studies of complexes between carboxylic acids and tertiary amines in argon matrices, *J.C.S. Faraday II* 76 (1980) 834-843.
- [21] S.E. Friberg, W.M. Sun, Y. Yang, A.J.I. Ward, Molecular interactions in nonaqueous cationic system, *J. Colloid Interface Sci.* 11 (1990) 503-517.
- [22] J. Päivärinta, S. Karlsson, A. Poso, M. Hotokka, Calculated molecular properties for different alkanolic acid-alkylamine complexes: A comparison with measured FTIR and Raman spectra, *Chem. Phys.* 263 (2001) 127-138.
- [23] K. Orzechowski, M. Pajdowska, K. Fuchs, U. Kaatze, Complex formation in binary propionic acid-triethylamine mixtures: A dielectric relaxation and titration study, *J. Chem. Phys.* 119 (2003) 8558-8566.
- [24] K. Orzechowski, M. Pajdowska, M. Czarnecki, U. Kaatze, Complexation and proton transfer in the binary system propionic acid-triethylamine, evidence from the composition dependencies of mixture properties, *J. Mol. Liq.* 133 (2007) 11-16.
- [25] G. M. Barrow, E. A. Yerger, Acid-base reactions in non-dissociating solvents. Acetic acid and triethylamine in carbon tetrachloride and chloroform, *J. Am. Chem. Soc.* 76 (1954) 5211-5216.

- [27] S. R. Gough, A. H. Price, Dielectric study of the molecular complexes formed between triethylamine and acetic acid and monochloroacetic acid, *J. Phys. Chem.* 72 (1968) 3347-3349.
- [26] D. F. DeTar, R. W. Novak, Carboxylic acid-amine equilibria in nonaqueous solvents, *J. Am. Chem. Soc.* 92 (1970) 1361-1365.
- [28] M. Padjowska, L. Sobczyk, Dielectric relaxation in propionic acid-tri-n-butylamine system, *Ad. Mol. Relax. Interact. Processes* 22 (1982) 159-165.
- [29] N. Nakanishi, H. Morita, S. Nagakura, Charge-transfer bands observed with the intermolecular hydrogen-bonded systems between acetic acid and some aliphatic amines, *J. Mol. Spectrosc.* 65 (1977) 295-305.
- [30] T. Liljefors, P. O. Norby, An ab initio study of the trimethylamine-formic acid and trimethylammonium ion-formate anion complexes, their monohydrates, and continuum solvation, *J. Am. Chem. Soc.* 119 (1997) 1052-1058.
- [31] N. Hafaiedh, A. Toumi, M. Bouanz, Dynamic viscosity study of binary mixtures triethylamine + water at temperatures ranging from (283.15 to 291.35) K, *J. Chem. Eng. Data* 54 (2009) 2195-2199.
- [32] H.S. van Klooster, W.A. Douglas, The system of acetic acid-triethylamine, *J. Phys. Chem.* 49 (1945) 67-70.

- [33] M. Bobik, Ultrasound absorption in mixtures of triethylamine with carboxylic acids, *Adv. Mol. Relax Interact. Processes* 11 (1977) 191-209.
- [34] J. Coates, Interpretation of infrared spectra, a practical approach, in: R.A. Meyers (Ed.), *Encyclopedia of Analytical Chemistry*, John Wiley & Sons Ltd, Chichester. 2000, pp. 10815-10837.
- [35] A. Burneau, F. Génin, F. Quilès, Ab initio study of the vibrational properties of acetic acid monomers and dimers, *Phys. Chem. Chem. Phys.* 2 (2000) 5020-5029.
- [36] R. Meyer, T. K. Ha, H. Frei, H. H. Günthard, Acetic acid monomer: Ab initio study, barrier to proton tunneling, and infrared assignment, *Chem. Phys.* 9 (1975) 393-403.
- [37] G. Socrates, *Infrared Characteristic Group Frequencies*, Wiley London: Chapman and Hall, New York, 1980.
- [38] S. Karlsson, S. Backlund, R. Friman, Complexation in the heptanoic acid-heptylamine system, *Colloid Polym. Sci.* 278 (2000) 8-14.
- [39] C. F. Gerald, *Applied Numerical Analysis*, Addison-Wesley Publishing Company, United States, 1970.

Figure captions

Fig. 1. The possible structures of the A_1C_1 , A_1C_2 and A_1C_3 TEA-acetic acid complexes.

Fig. 2. Phase diagram of TEA-acetic acid binary mixtures; \diamond indicates LLE data obtained by Kohler and coworkers [12]; \circ LLE data, and \blacklozenge & \triangle VLE data obtained by van Klooster and Douglas [32] at atmospheric pressure; and \bullet LLE data obtained in the present study.

Fig. 3. Liquid phase FTIR spectra of binary TEA-acetic acid mixtures in comparison with pure acetic acid and pure TEA.

Fig. 4. DSC profiles of TEA-acetic acid binary mixtures in comparison with pure acetic acid and pure TEA.

Fig. 5. TG-FTIR data for heating sodium bicarbonate from 25 °C to 400 °C at a scan rate of 20 °C min⁻¹ in nitrogen gas flowing at a rate of 50 mL min⁻¹. It plots the maximum absorbance of the band located near 2300 wavenumbers in the FTIR spectrum (\square) and the TG derivative mass signal shifted by a time interval of 0.56 min (\blacktriangle).

Fig. 6. TGA evaporation profiles of selected TEA-acetic acid binary mixtures compared to pure acetic acid and pure TEA.

Fig. 7. Time required to reach selected fractional mass loss values as a function of the initial composition of the mixture.

Fig. 8. Time evolution of the gas phase FTIR spectra for a mixture with initial composition $z_A = 0.89$ as a function of mass fraction evaporated. The arrow indicates the time direction and the spectra for pure TEA and pure acetic acid are shown for comparison.

Fig. 9. Time evolution of the gas phase FTIR spectra for a mixture with initial composition $z_A = 0.20$ as a function of mass fraction evaporated. The arrow indicates the time direction and the spectra for pure TEA and pure acetic acid are shown for comparison.

Fig. 10. Shape functions α for pure acetic acid, pure TEA and experimental data (Δ) for a vapour mixture. The solid line for the mixture was generated using the equation (3) with the $\beta_{\text{mix}} = 0.638$ value determined via a least square curve fit. According to calculations utilizing Equations (4) and (5), this indicates that the mixture contained approximately 25 mol % amine.

Fig. 11. Time dependence of the mole fraction TEA present in the released vapor. The indicated TEA concentrations refer to the initial TEA content of the liquid phase.

Fig. 12. Mole fraction TEA released into the vapor phase as a function of the fraction mixture released. The indicated TEA concentrations refer to the initial TEA content of the liquid phase.

Fig. 13. Calculated mole fractions of TEA in the liquid phase as a function of the initial mixture composition and the fraction mixture released. The indicated TEA concentrations refer to the initial content of the liquid phase.

Figures

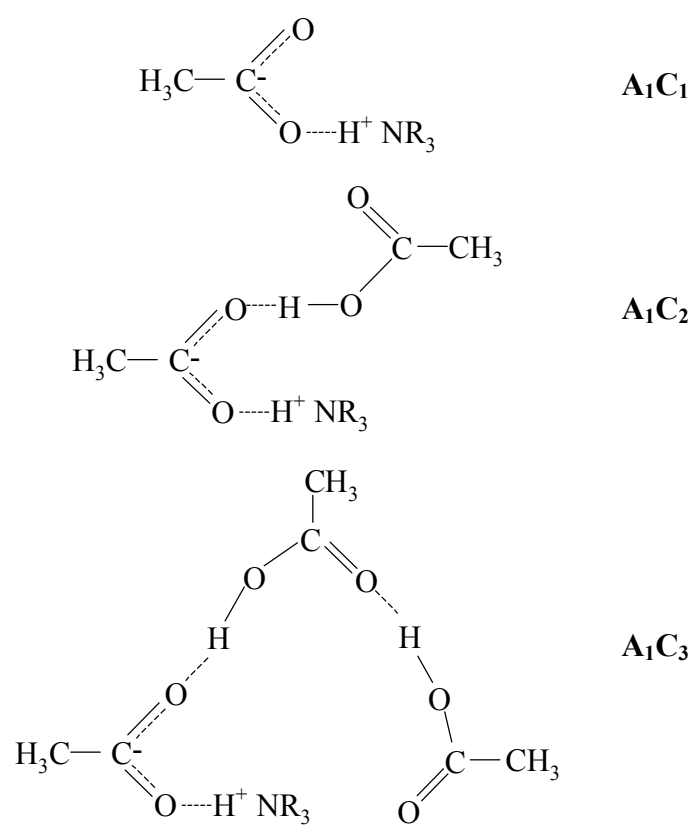


Fig. 1.

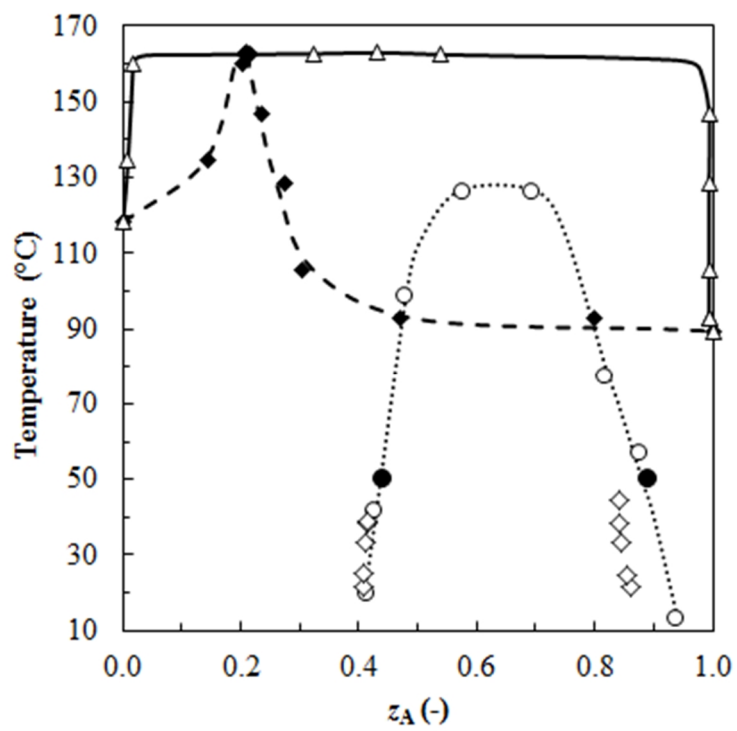


Fig. 2.

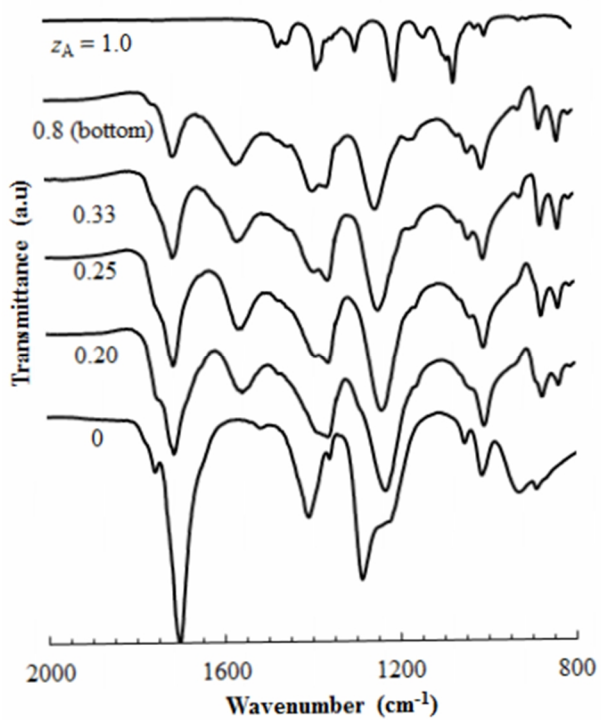


Fig. 3.

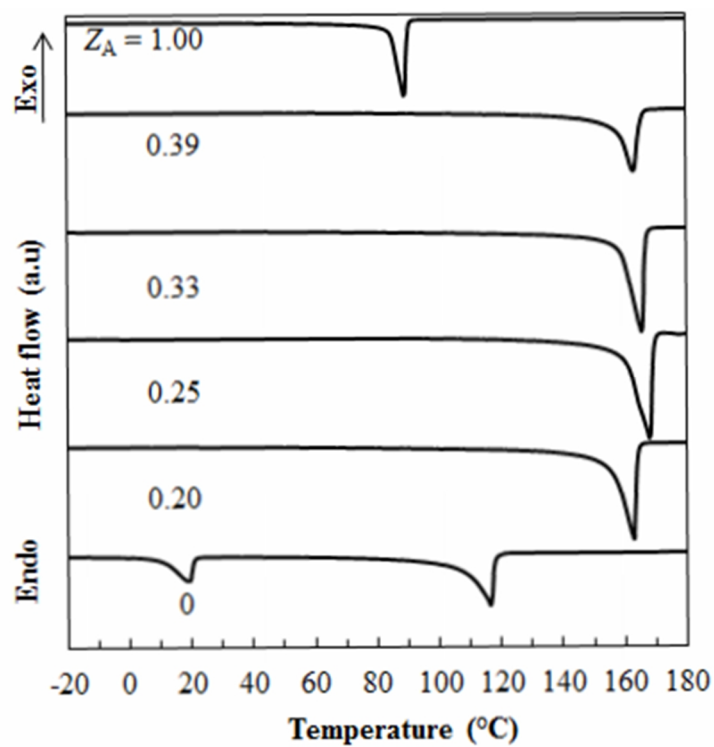


Fig. 4.

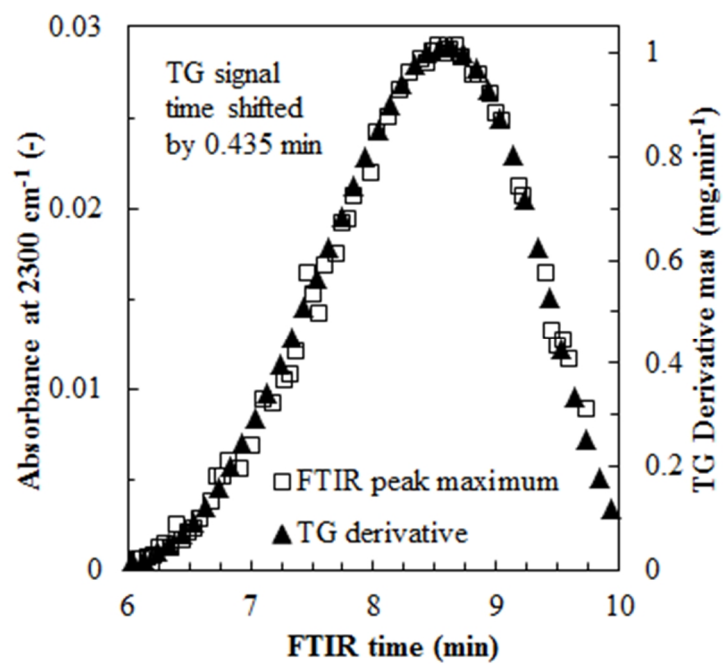


Fig. 5.

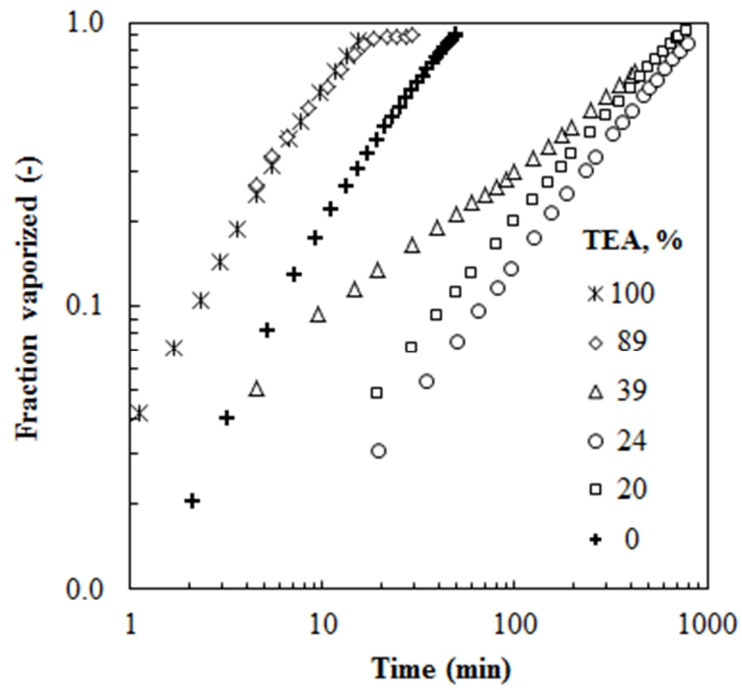


Fig. 6.

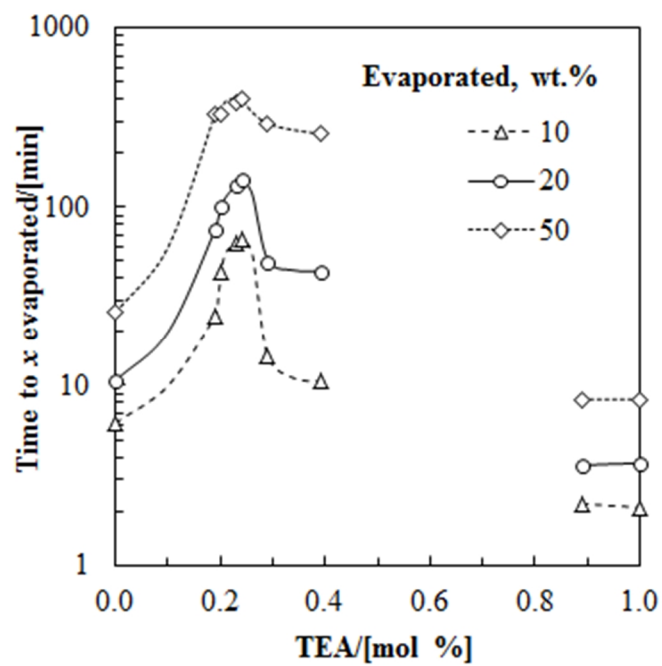


Fig. 7.

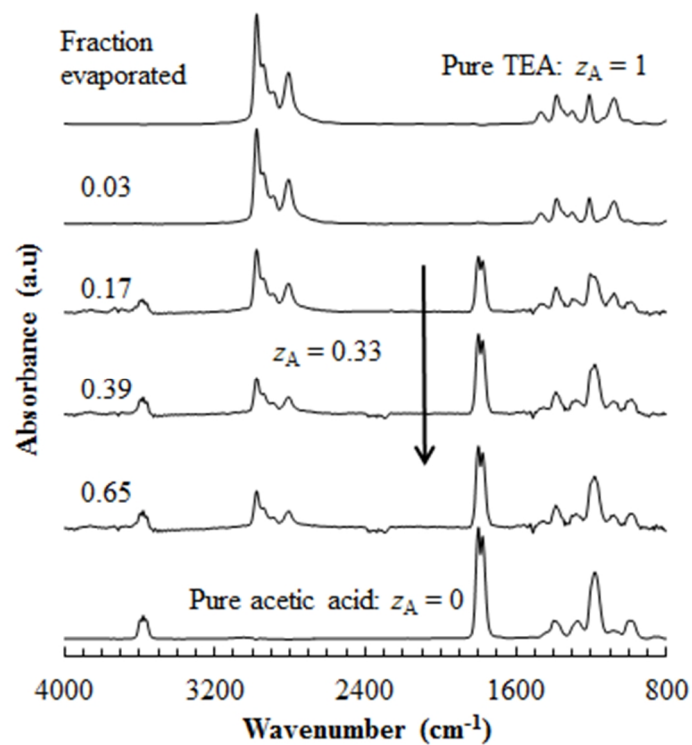


Fig. 8.

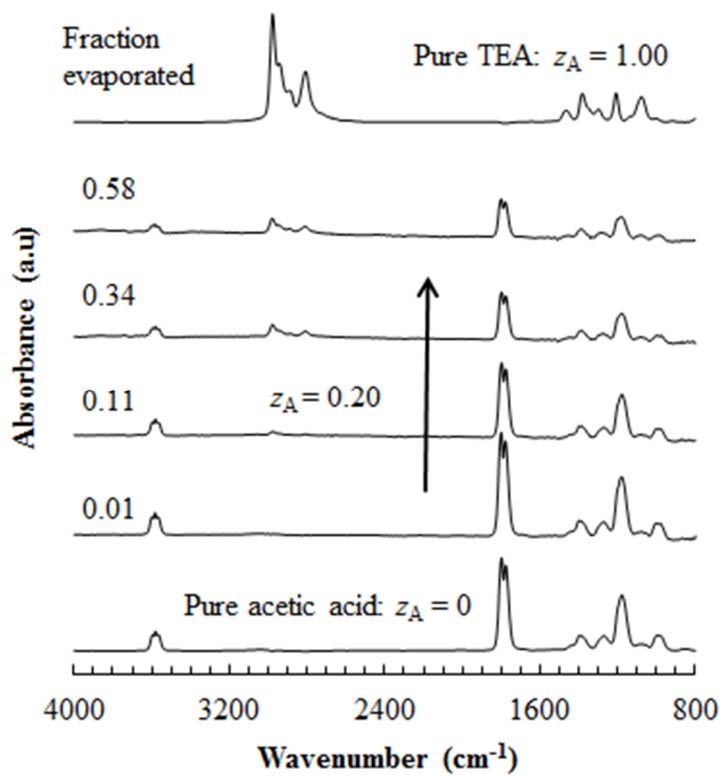


Fig. 9.

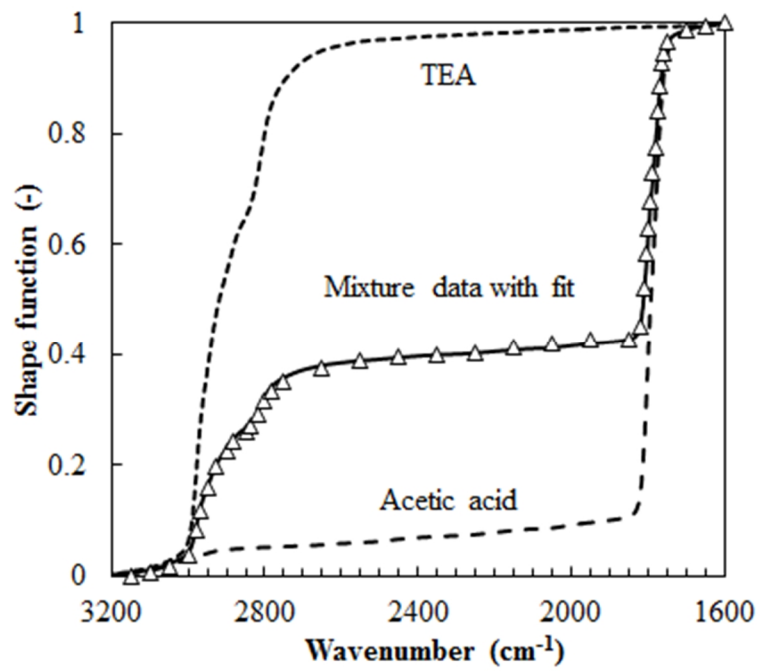


Fig. 10.

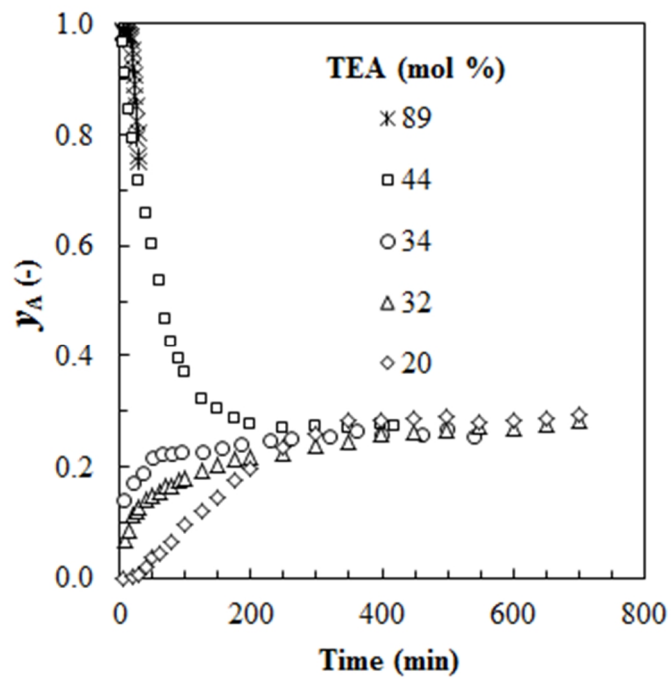


Fig. 11.

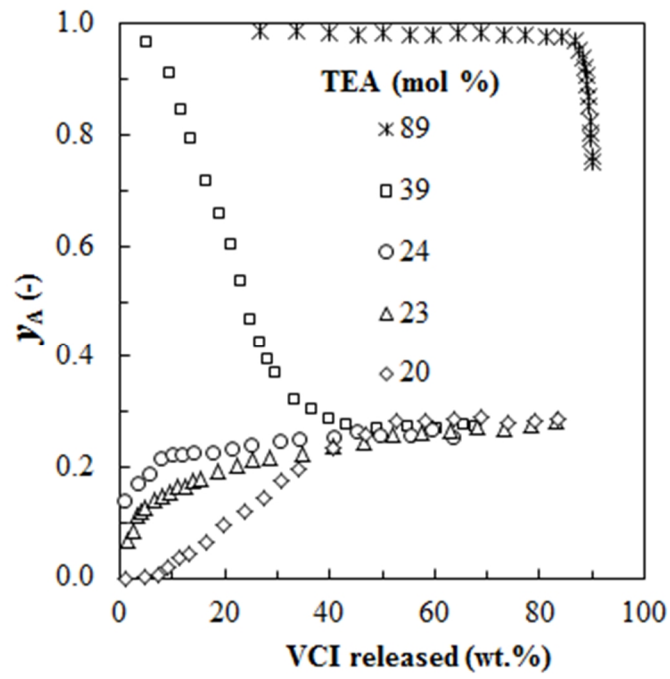


Fig. 12.

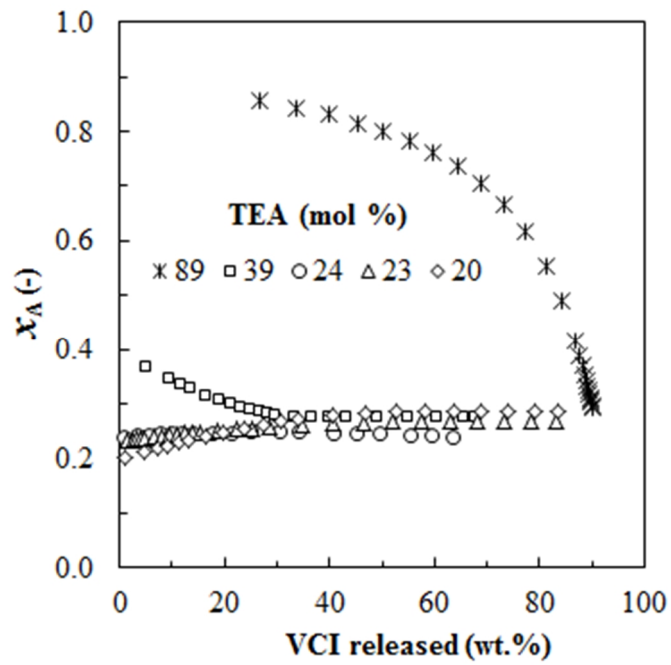


Fig. 23.